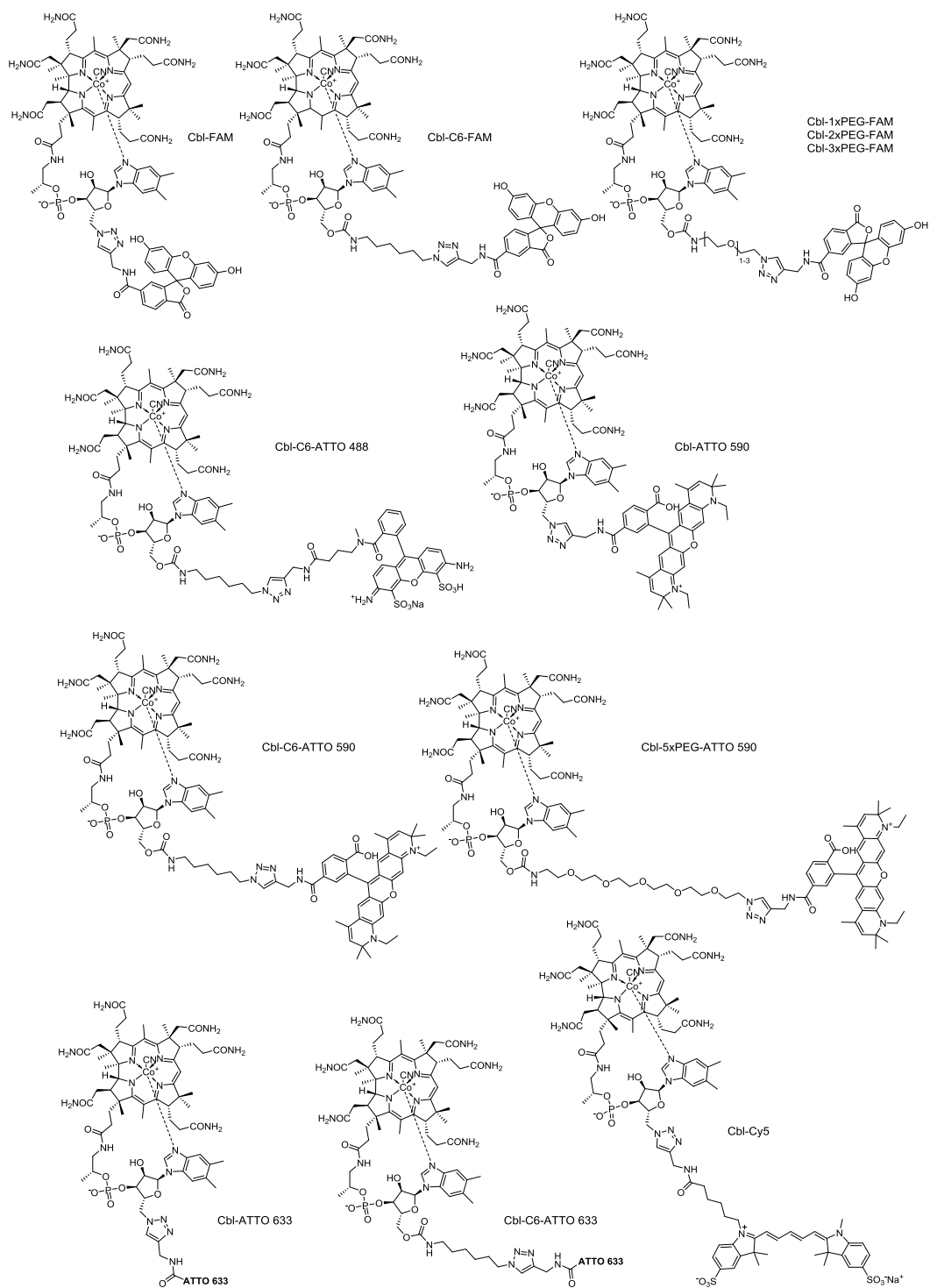


Supporting Information

Development of a riboswitch-based platform for live cell imaging of RNAs in mammalian cells

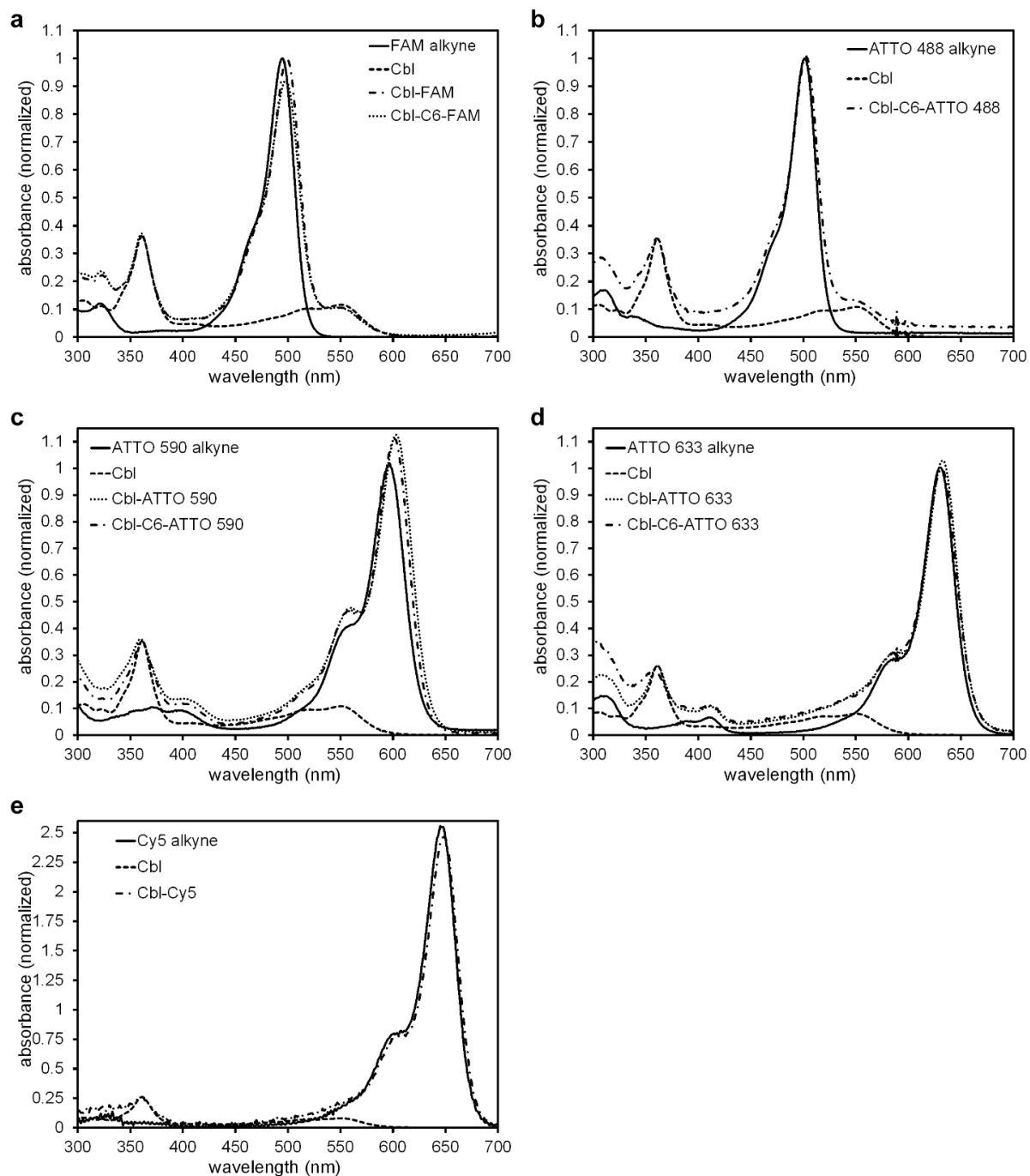
| | |
|-------------------------------|----|
| Supplementary Figures | 2 |
| Supplementary Figure 1 | 2 |
| Supplementary Figure 2 | 3 |
| Supplementary Figure 3 | 4 |
| Supplementary Figure 4 | 5 |
| Supplementary Figure 5 | 6 |
| Supplementary Figure 6 | 7 |
| Supplementary Figure 7 | 8 |
| Supplementary Figure 8 | 9 |
| Supplementary Figure 10 | 11 |
| Supplementary Figure 11 | 12 |
| Supplementary Figure 12 | 13 |
| Supplementary Figure 13 | 14 |
| Supplementary Figure 14 | 15 |
| Supplementary Figure 15 | 17 |
| Supplementary Figure 16 | 18 |
| Supplementary Figure 17 | 19 |
| Supplementary Figure 18 | 20 |
| Supplementary Figure 19 | 21 |
| Supplementary Tables | 22 |
| Supplementary Table 1 | 22 |
| Supplementary Table 2 | 23 |
| Supplementary Table 3 | 24 |
| Supplementary Table 4 | 25 |
| Supplementary Table 5 | 26 |

Supplementary Figures



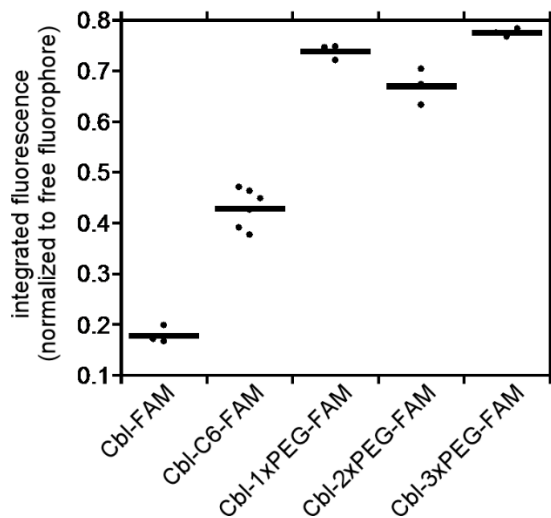
Supplementary Figure 1

Chemical structures of probes used in this study.



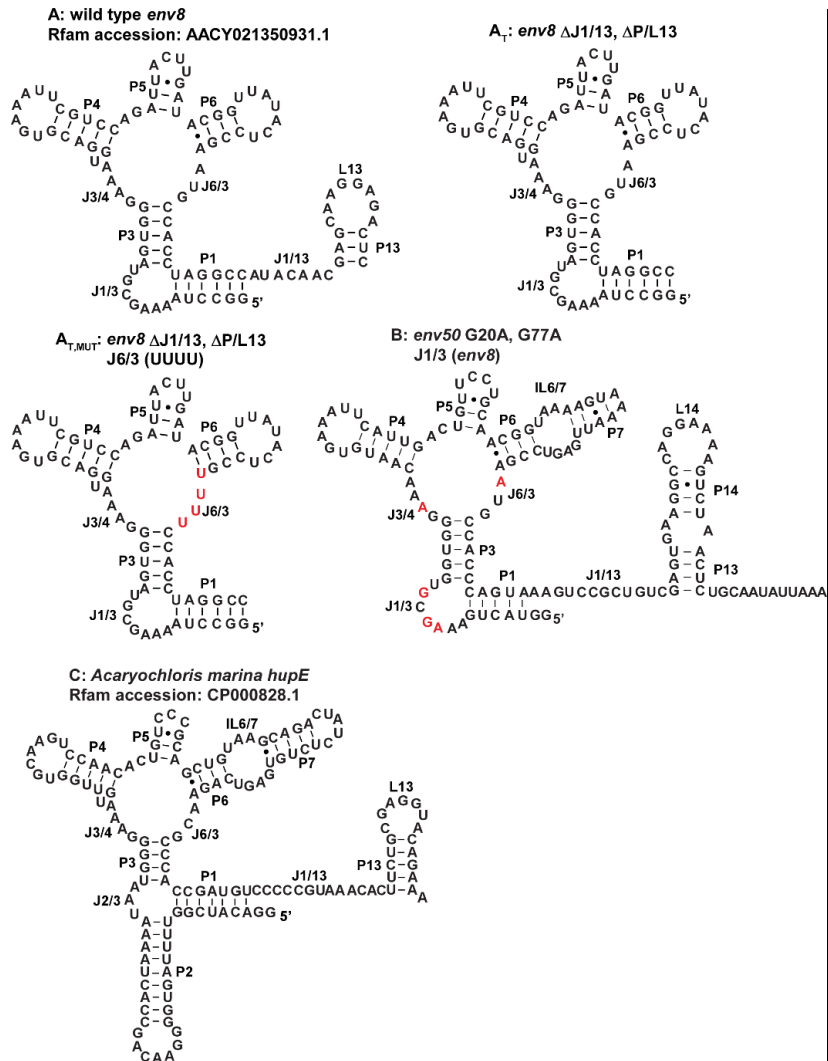
Supplementary Figure 2

Absorbance spectra of representative Cbl-fluorophore probes in comparison to the spectra of free Cbl and each fluorophore. The absorbance intensities were normalized to the maximum absorbance peak of Cbl at 361 nm to allow for evaluation of changes in absorbance peak shapes.



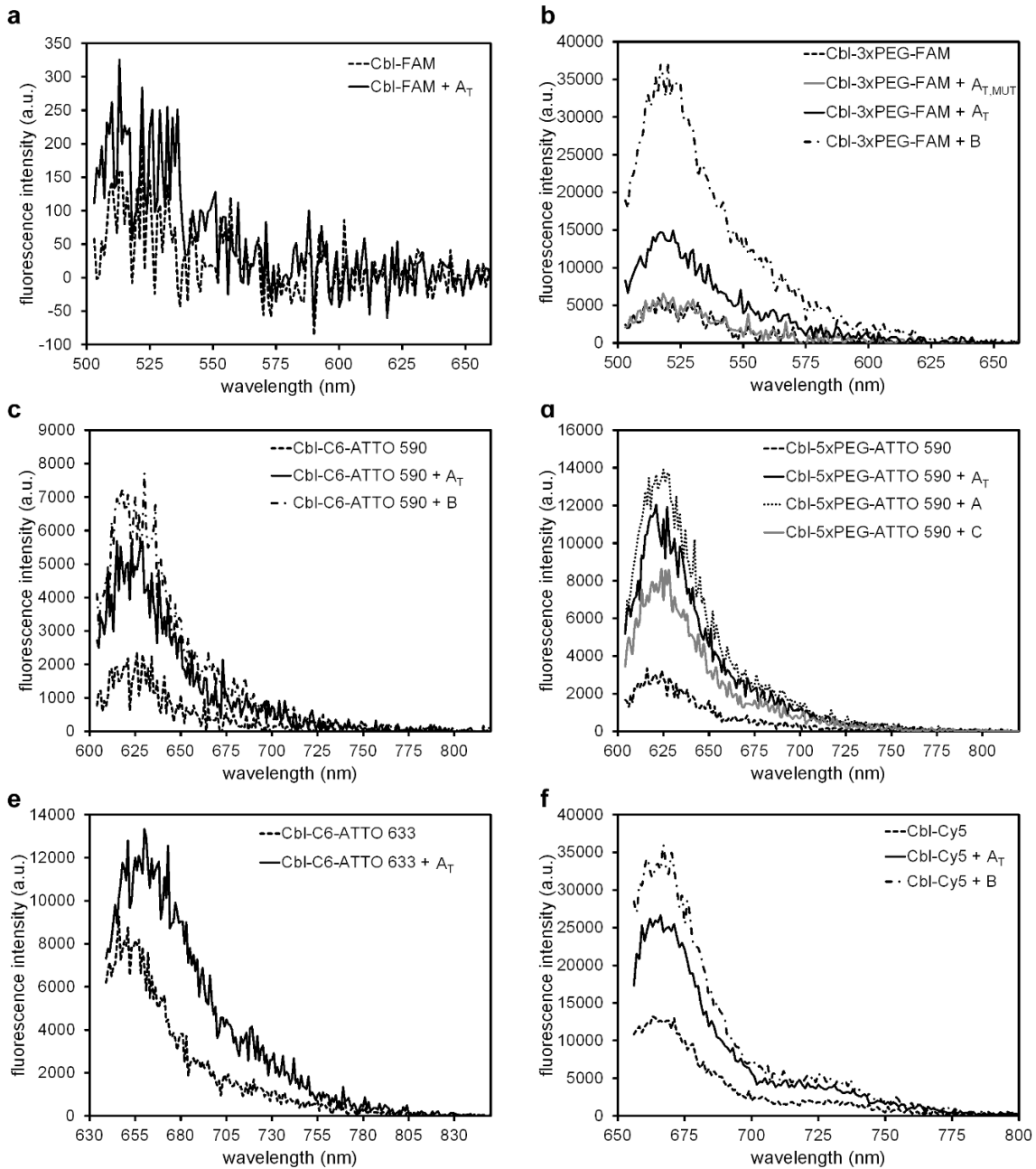
Supplementary Figure 3

Comparison of residual fluorescence for Cbl-FAM probes with varied linkers. The fluorescence was quantified and compared to the signal of the free fluorophore at the same concentration as in Figure 1d. The mean for at least $n = 3$ independent measurements is shown.



Supplementary Figure 4

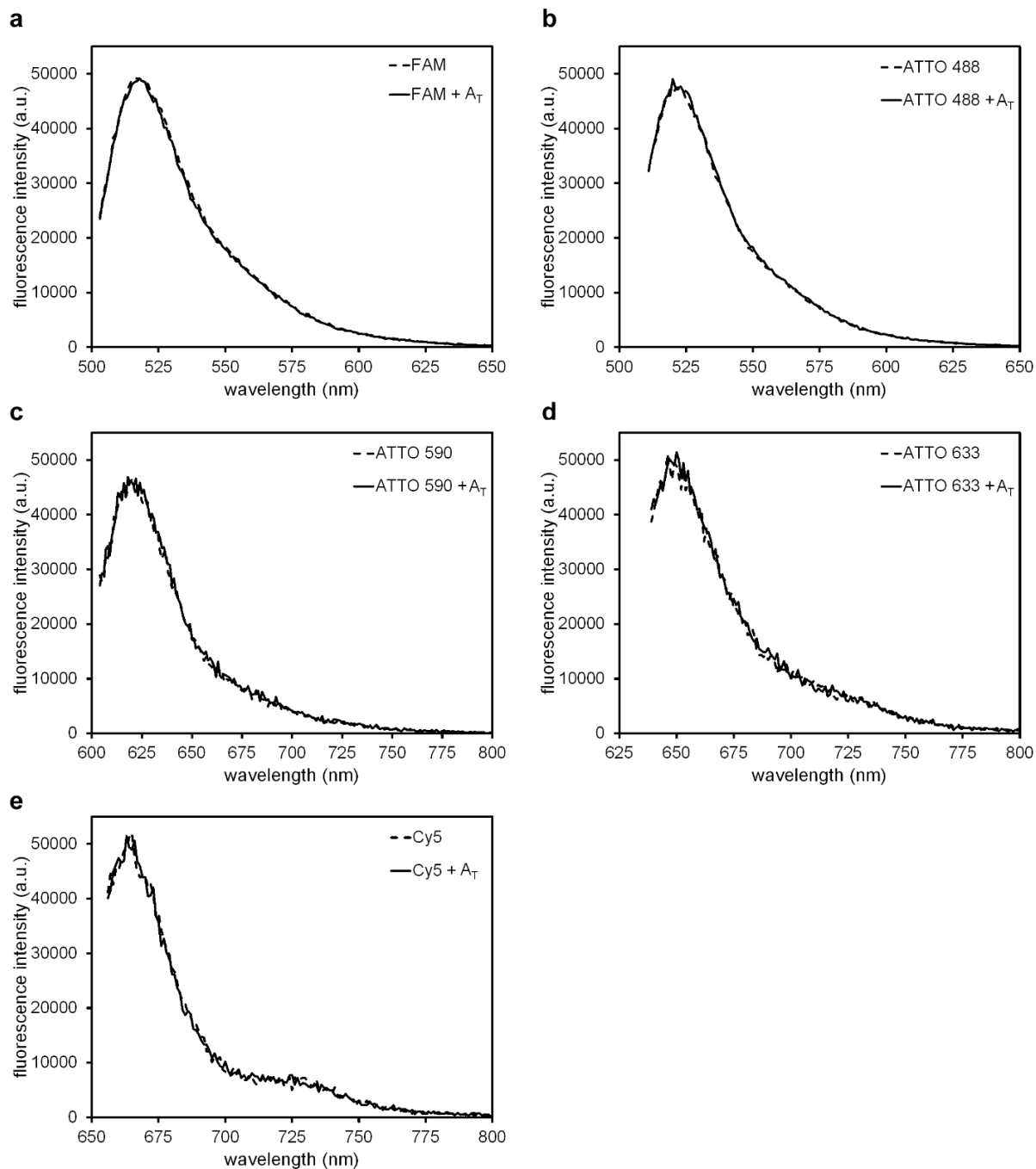
Secondary structures of RNAs used in this study with key structural regions denoted as P (paired), J (junction), L (loop), and IL (internal loop). Naturally derived sequences are shown with accompanying Rfam accession numbers, and the secondary structure of wild type *env8* (variant A) is based on crystallographic data²⁶. Nucleotides that are colored red in variant A_{T,MUT} represent point mutations made to the binding core of wild type *env8* that abrogate cobalamin binding. Nucleotides that are colored red in variant B represent point mutations derived from wild type *env8* that have been shown to increase the affinity of this RNA⁴⁴ for forms of cobalamin similar to the conjugates used in this study. Features that induce bulkiness of the RNA include P13 for variant A, P7, P13, P14 for variant B and P7, P2, P13 for variant C.



Supplementary Figure 5

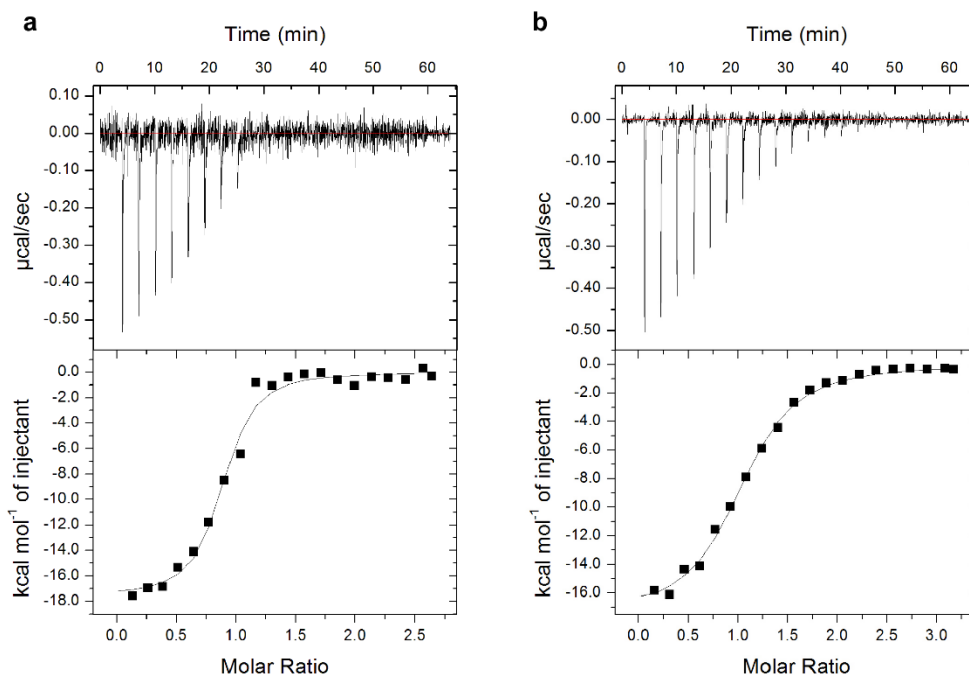
Representative fluorescence spectra of Cbl-fluorophore probes in the presence and absence of aptamers used in this study (see also Supplementary Table 1 for photophysical properties).

Spectra show an increase in fluorescence intensity upon binding RNA aptamer A, A_T , B, or C but not the non-binding aptamer $A_{T,MUT}$. Triplicates of spectra shown here were used to generate the bar graphs presented in Figure 2.



Supplementary Figure 6

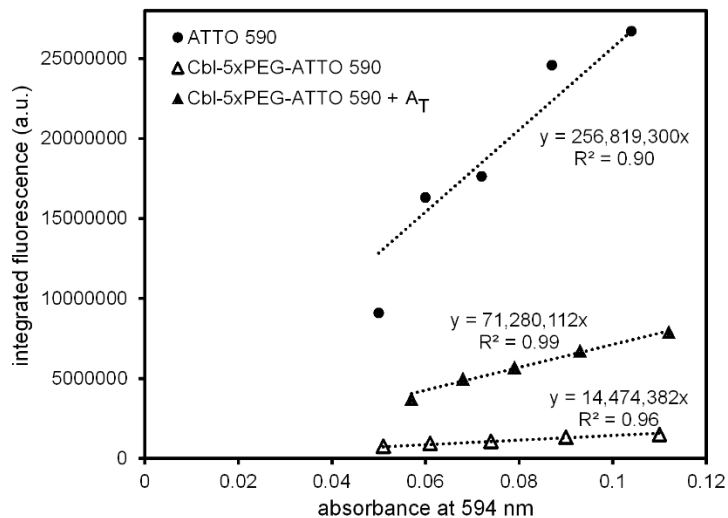
Representative fluorescence spectra of free fluorophores used in this study in the presence and absence of aptamer A_T . Spectra reveal no change in fluorescence intensity of free fluorophores in the presence of aptamer A_T . Triplicates of spectra shown here were used to generate the bar graphs presented in Figure 1.



| Cbl variant | Cbl | Cbl-5xPEG-ATTO 590 |
|-------------------------|-----------------|--------------------|
| K_D (μM) | 0.29 ± 0.10 | 1.3 ± 0.56 |

Supplementary Figure 7

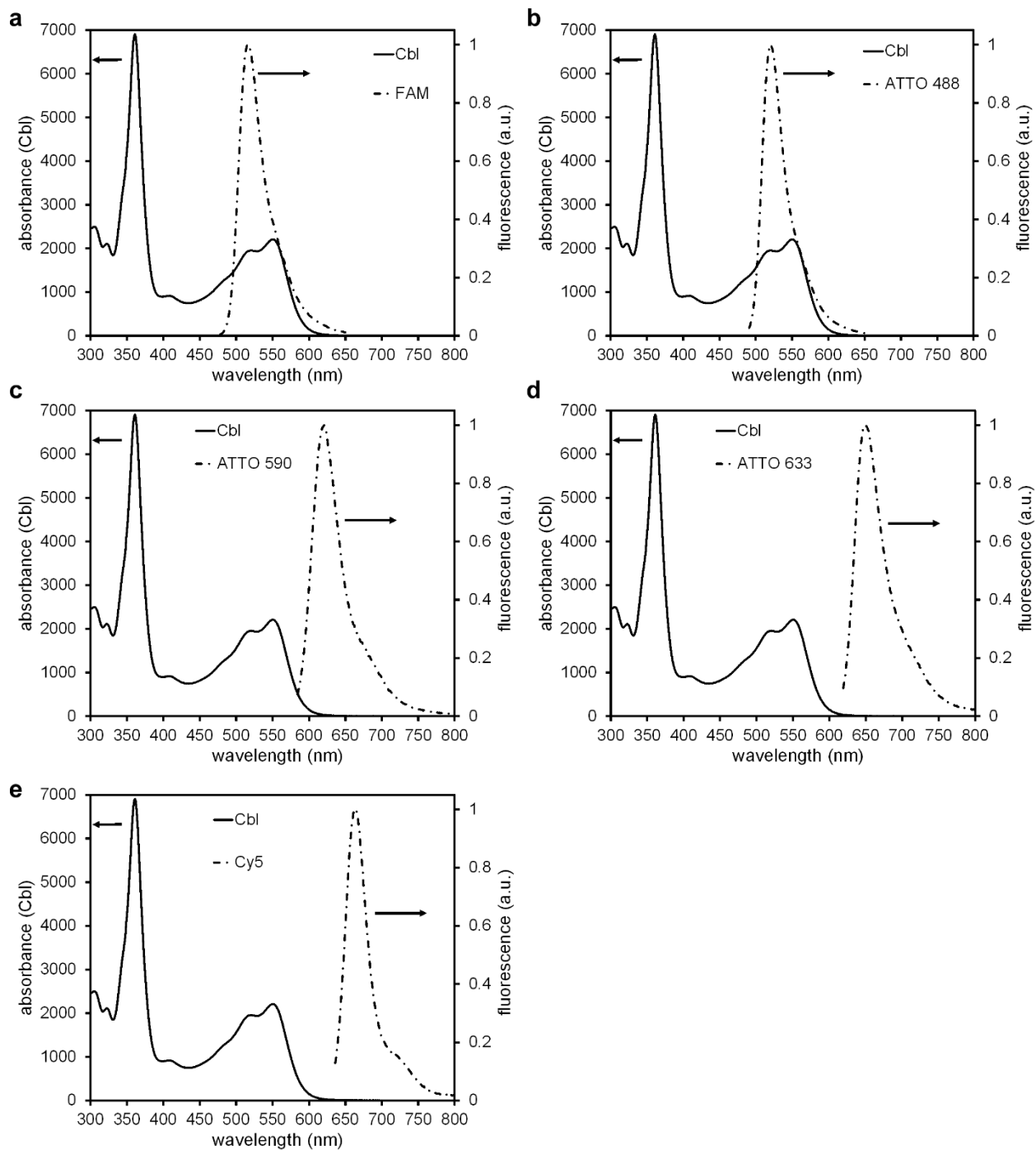
The aptamer A_T binds to the probe Cbl-5xPEG-ATTO 590 with an affinity that is comparable with binding of A_T to Cbl. Representative isothermal titration calorimetry thermograms of the aptamer A_T binding to Cbl (a) and Cbl-5xPEG-ATTO 590 (b). K_D reported is the mean of 3 independent experiments +/- SDEV.



| | Quantum yield Q |
|-------------------------------------|-----------------|
| ATTO 590 | 0.8 (Atto tec) |
| Cbl-5xPEG-ATTO 590 | 0.05 |
| Cbl-5xPEG-ATTO 590 + A _T | 0.22 |

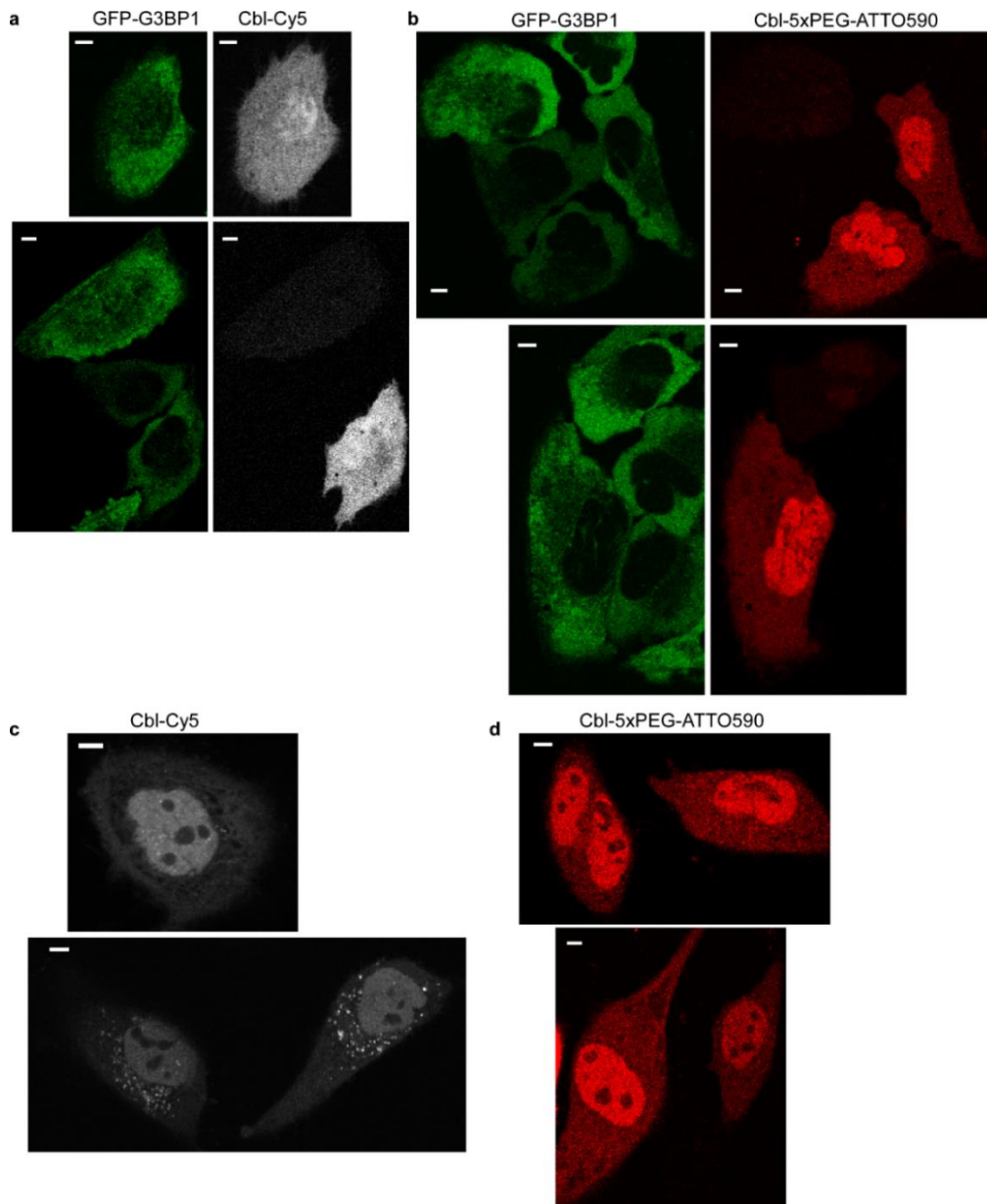
Supplementary Figure 8

Determination of the quantum yield for Cbl-5xPEG-ATTO 590 in the presence and absence of the aptamer A_T, compared with the quantum yield for ATTO590. The quantum yields from this measurement are reported.



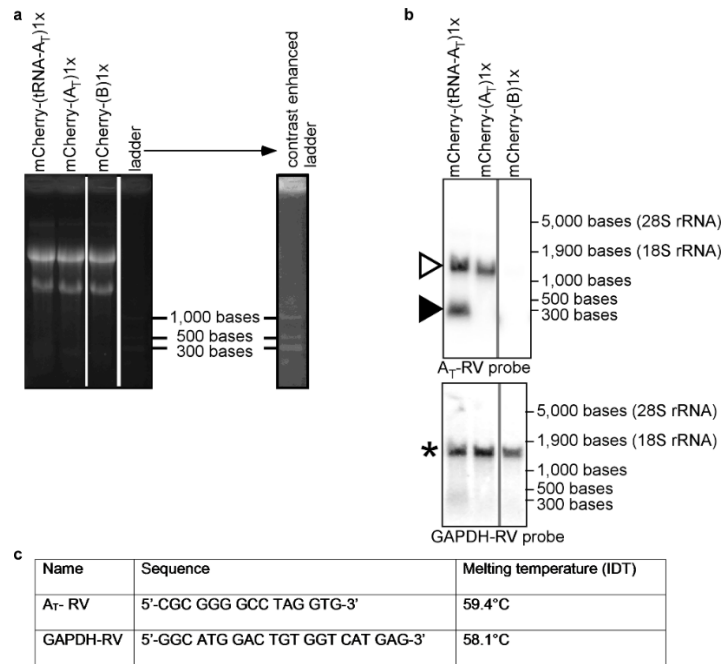
Supplementary Figure 9

Cbl absorbance spectra and fluorescence emission spectra of fluorophores to calculate the overlap integral $J(\lambda)$.



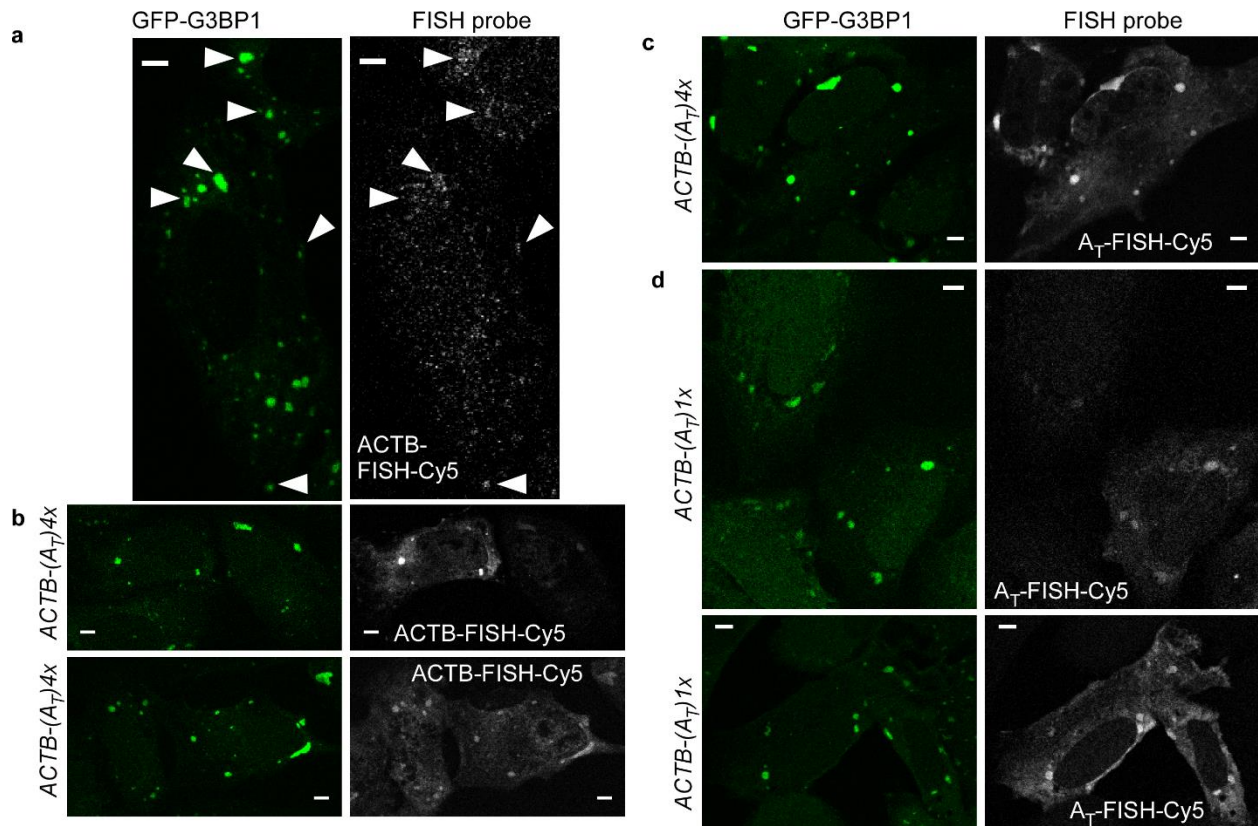
Supplementary Figure 10

Cbl-fluorophore probes distribute diffusely, consistent with cytosolic localization, in live mammalian cells after bead loading. (a) Cbl-Cy5 was bead loaded in U2-OS cells that stably produce the SG marker protein GFP-G3BP1 (1 experiment, 56 cells). (b) Cbl-5xPEG-ATTO590 was bead loaded in U2-OS cells that stably produce the SG marker protein GFP-G3BP1 (1 experiment, 49 cells). (c) Cbl-Cy5 was bead loaded in HeLa cells (2 experiment, 97 cells). (d) Cbl-5xPEG-ATTO 590 was bead loaded in HeLa cells (1 experiment, 65 cells).



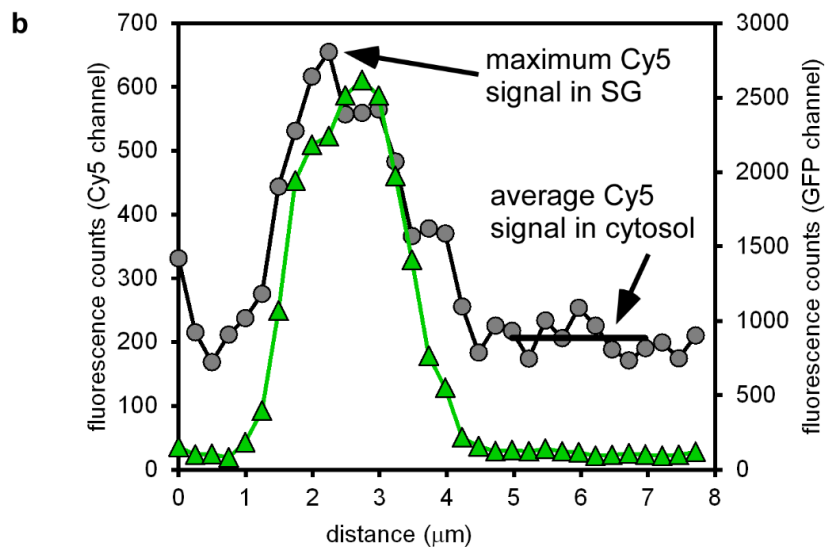
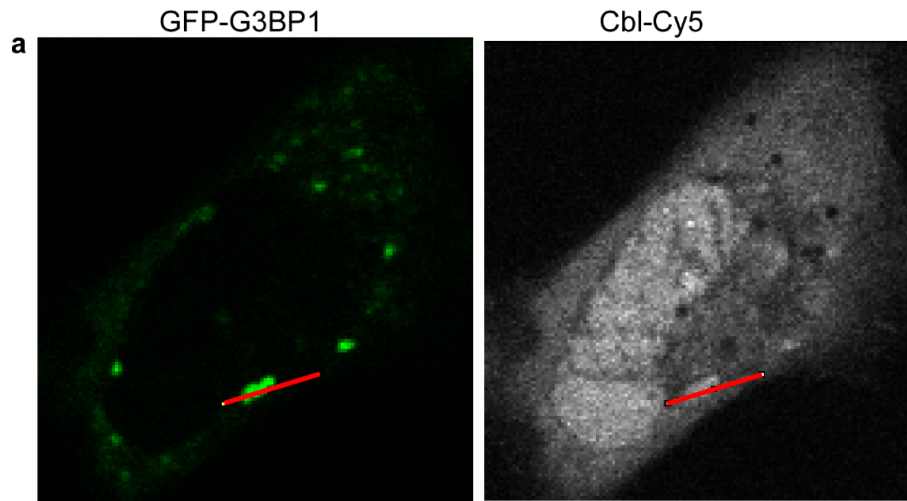
Supplementary Figure 11

mRNA can be tagged with the A_T aptamer without unwanted processing. 293T cells were transiently transfected with plasmid DNA where the A_T or B aptamer was genetically fused to a reporter mRNA (encoding mCherry). The aptamer A_T was produced with or without the tRNA folding scaffold. (a) Total RNA was separated by agarose gel electrophoresis. The 28S and 18S rRNA bands across samples serve as loading controls and indicate that no unwanted RNA processing occurred during RNA preparation. Non-consecutive lanes of the same gel are indicated by vertical lines. Contrast settings were identical for all parts of the gel. A contrast enhanced version of the lane with the RNA ladder is shown as a reference. (b) Northern blot probed against the A_T aptamer (top panel) indicates that the full length mRNA (open triangle) is processed when produced with the tRNA folding scaffold (filled triangle). The blot was stripped and probed for GAPDH mRNA (star in bottom panel). Non-consecutive lanes of the same blot are indicated by vertical lines. No changes were made to contrast settings after cropping lanes. (c) Properties of oligos from (b). The tRNA processing phenotype was reproducible for two independent experiments.



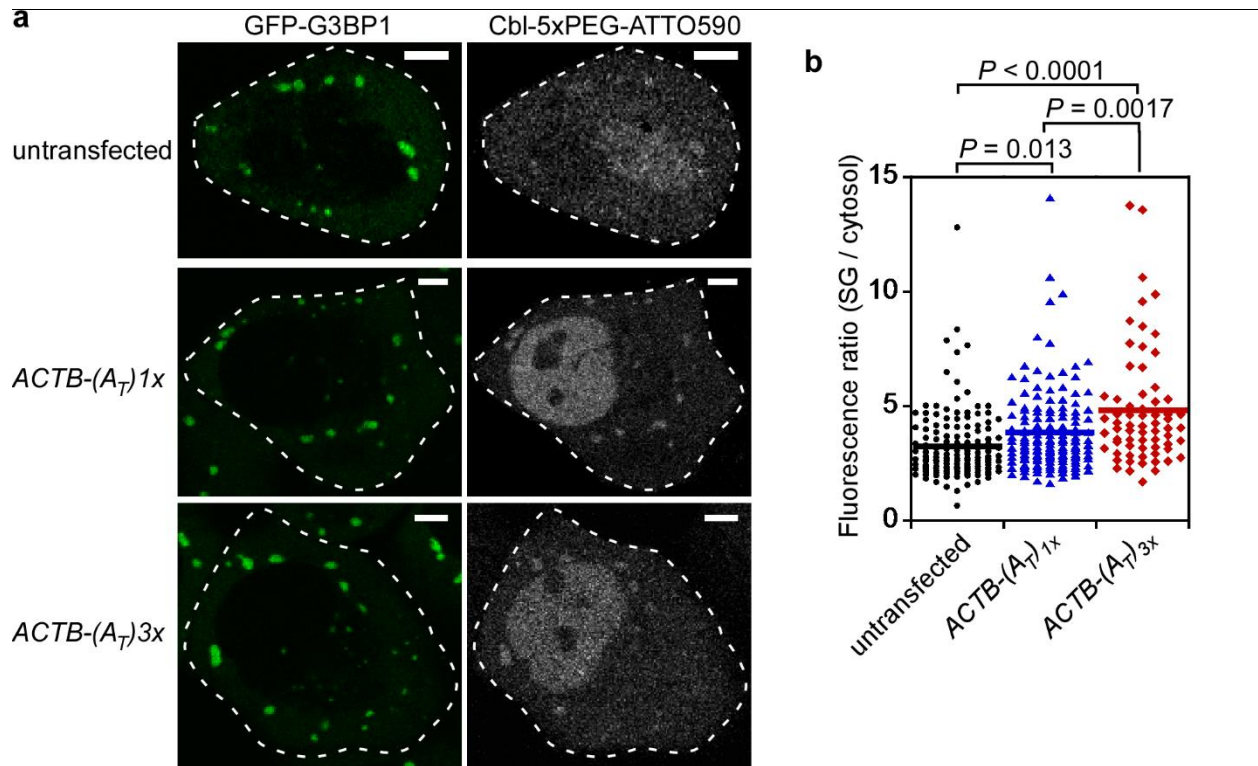
Supplementary Figure 12

ACTB mRNA colocalizes with GFP-G3BP1, a marker protein for SGs in U2-OS cells. Detection of endogenous ACTB mRNA (a) or transiently transfected *ACTB-(A₇)_{4x}* (b, c) or *ACTB-(A₇)_{1x}* (d) in U2-OS cells that stably produce GFP-G3BP1, a SG marker protein. Cells were fixed, permeabilized and ACTB fusion mRNA was visualized by FISH using a Cy5-conjugated probe. (a) Representative cells show localization of ACTB mRNA to SGs (1 experiment, 15 cells). (b) Two representative images showing localization of ACTB mRNA to SGs using a FISH probe against the ACTB portion of the mRNA fusion (1 experiment, 25 cells). (c) Representative image showing localization of *ACTB-(A₇)_{4x}* mRNA to SGs using a FISH probe against A₇ (1 experiment, 10 cells). (d) Representative image showing localization of *ACTB-(A₇)_{1x}* to SGs using a FISH probe against A₇ (1 experiment, 25 cells). Scale bar = 5 μm



Supplementary Figure 13

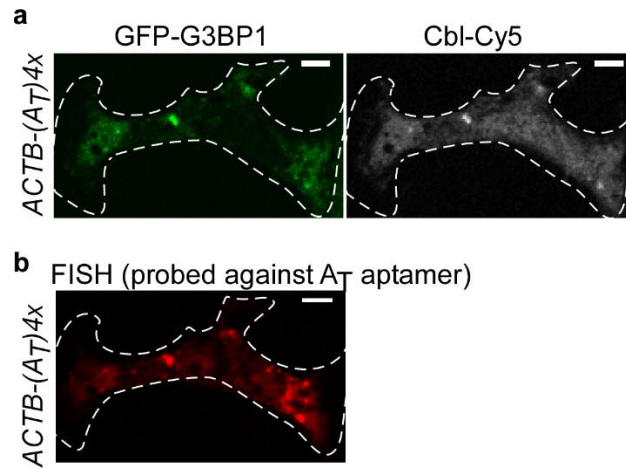
Analysis of live U2-OS SG cells to quantify Cbl-fluorophore probe fluorescence in SGs. (a) SGs were identified in the GFP channel and a line trace was drawn through the SG including cytosolic fluorescence near the SG. The same signal trace was recorded in the probe fluorescence channel (in this case Cbl-Cy5). (b) After background subtraction, the Cbl-fluorophore probe fluorescence trace as well as the control GFP-G3BP1 trace were plotted. The maximum fluorescence signal for the Cbl-fluorophore probe was determined and divided by the average probe fluorescence in the cytosol.



Supplementary Figure 14

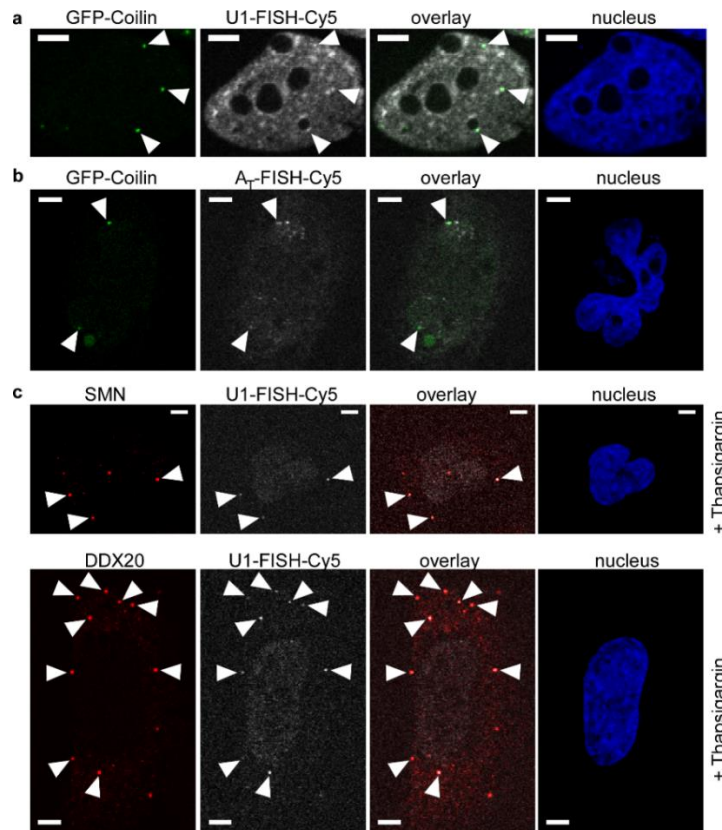
Cbl-5xPEG-ATTO590 fluorescence signal increased in SGs in cells that were transiently transfected with *ACTB-A_T* fusion constructs. (a) Live cell microscopy images of U2-OS cells, stably producing GFP-G3BP1 as a marker protein for SGs, in both the GFP channel (green, labelled GFP-G3BP1) and ATTO590 channel (black and white). Cells were transiently transfected with the indicated plasmids producing ACTB mRNA tagged with the aptamer A_T. The probe Cbl-5xPEG-ATTO590 was introduced into cells by bead loading 24 h post transfection, SG formation was induced by treatment with 0.5 mM arsenite for 45 min, followed by live cell microscopy. (b) Fluorescence increase for Cbl-5xPEG-ATTO590 in SGs was quantified by collecting a line trace through each SG (identified in the GFP channel) and calculating the ratio of the highest signal in the SG over the average signal in the cytosol (see Supplementary Figure 12 for details). Untransfected: 2 independent experiments, 51 cells, 144 SGs. *ACTB-(A_T)1x*: 2 independent experiments, 64 cells, 150 SGs. *ACTB-(A_T)3x*: 2

independent experiments, 27 cells, 67 SGs, one way ANOVA (95% confidence limit), post hoc test (Tuskey HSD), scale bar = 5 μm .



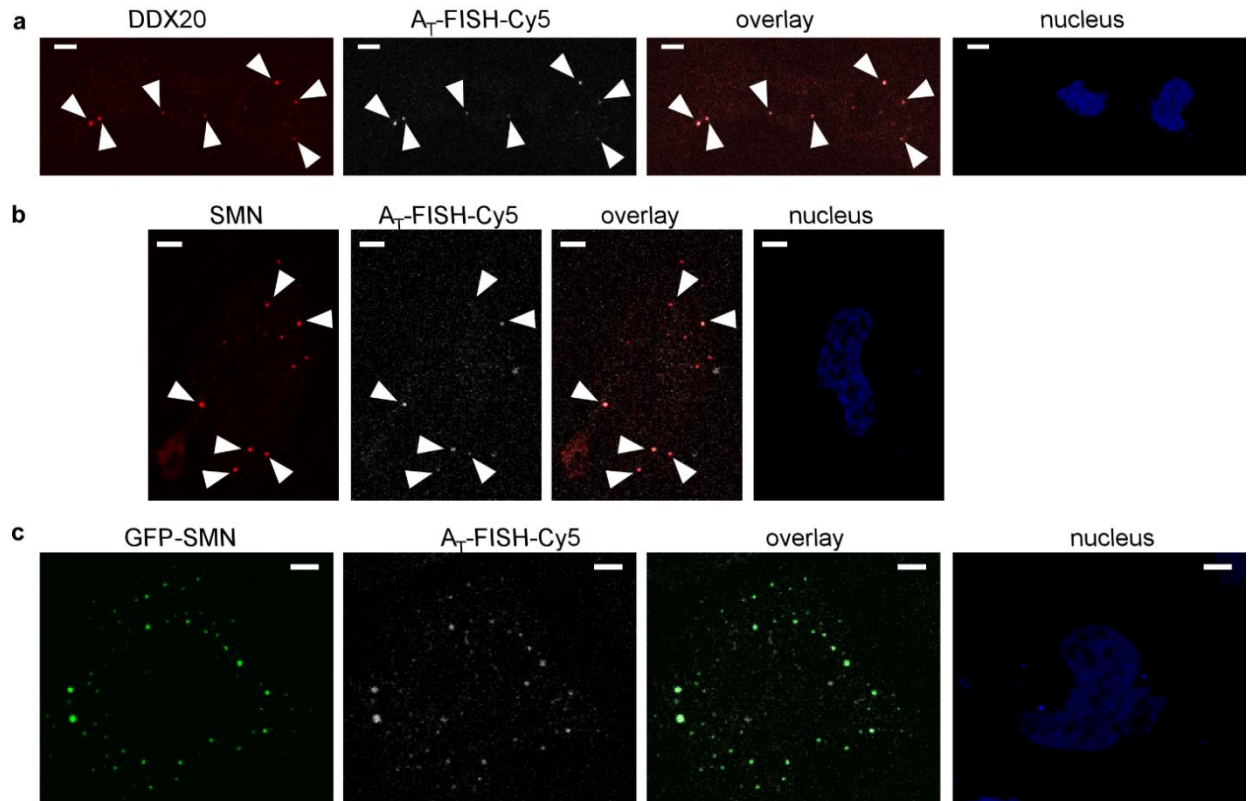
Supplementary Figure 15

Correlative fluorescence microscopy of live (a) and fixed cells (b) confirms colocalization of ACTB mRNA to SGs. (a) Fluorescence of Cbl-Cy5 colocalized with SGs. (b) After fixation, localization of the A_T tag to SGs was directly assessed by FISH (2 experiments, 4 cells). Scale bar = 5 μ m.



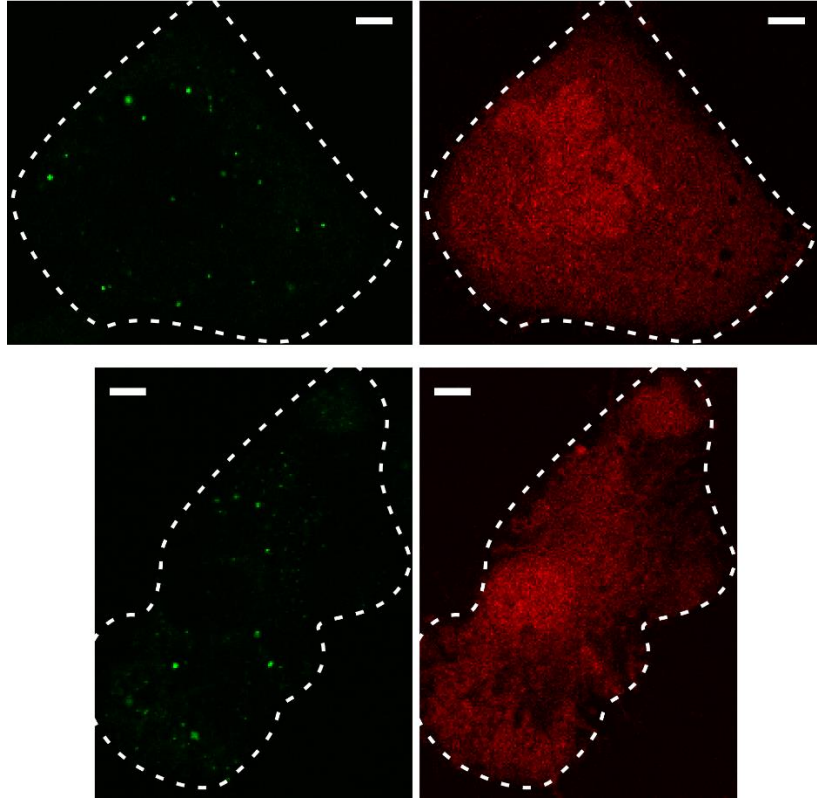
Supplementary Figure 16

Localization phenotypes of U1 snRNA in normal and Thapsigargin-stressed HeLa cells. (a) Endogenous U1 snRNA colocalizes with nuclear Coilin-containing foci. HeLa cells were transiently transfected with a plasmid to produce GFP-Coilin, fixed and permeabilized. U1 snRNA was visualized via a probe against the U1 snRNA coding sequence (1 experiment, 6 cells). (b) A_T-U1 RNA can localize to Coilin-containing nuclear foci. HeLa cells were transiently transfected with two plasmids to produce GFP-Coilin and A_T-U1 snRNA, fixed and permeabilized. A_T-U1 snRNA was visualized via a probe against the A_T aptamer (2 experiments, 3 cells). (c) Endogenous U1 snRNA colocalizes with two marker proteins for U-bodies, endogenous SMN (1 experiment, 5 cells) and endogenous DDX20 (1 experiment, 9 cells), upon Thapsigargin treatment. HeLa cells were fixed and permeabilized. U1 snRNA was visualized via a probe against U1, and DDX20 and SMN were visualized by immunofluorescence. Scale bar = 5 μm.



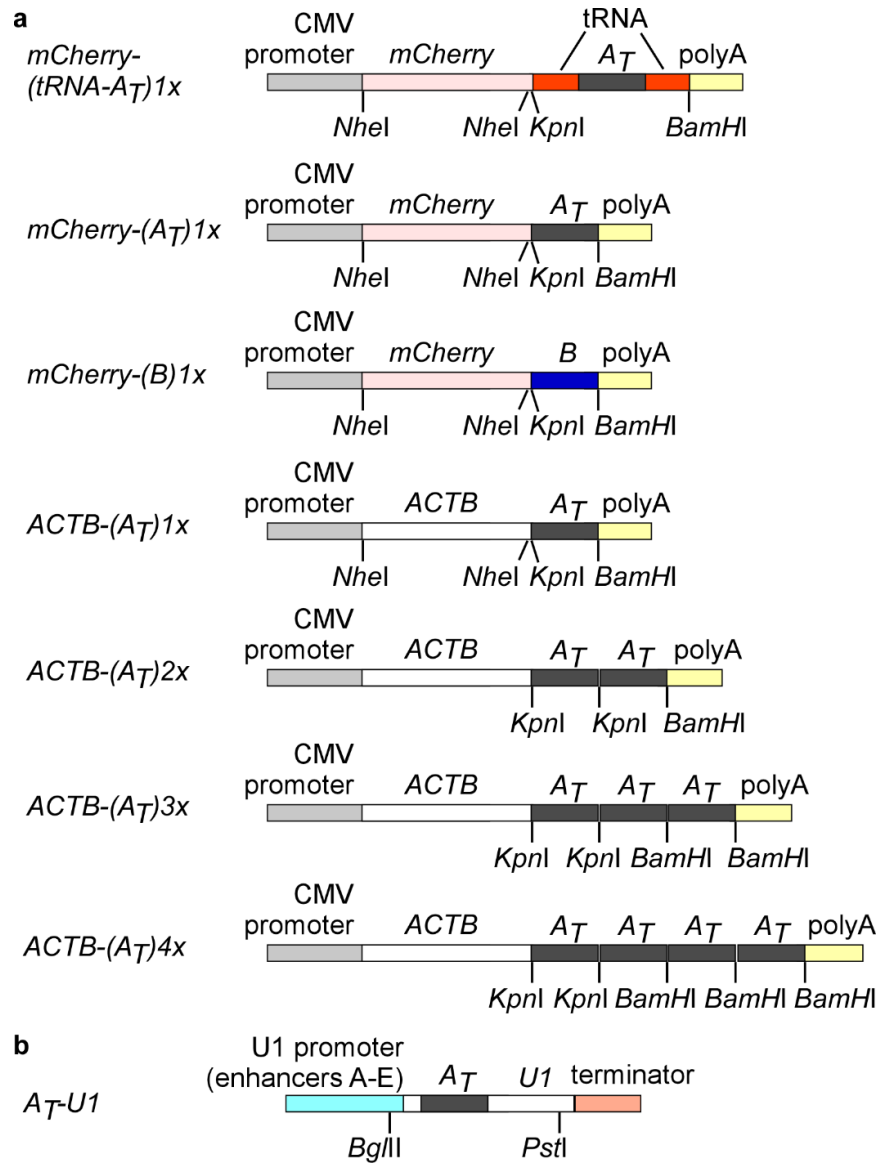
Supplementary Figure 17

Transiently transfected U1 snRNA tagged with aptamer A_T can localize to U-body marker proteins DDX20 and SMN. (a) A_T -U1 snRNA can colocalize with the U-body marker protein DDX20 after treatment of cells with Thapsigargin. A_T -U1 snRNA was visualized via an A_T aptamer specific probe and endogenous DDX20 was detected by immunofluorescence (1 experiment, 12 cells). (b) A_T -U1 snRNA can colocalize with the U-body marker protein SMN after treatment of cells with Thapsigargin. A_T -U1 snRNA was visualized via an A_T aptamer specific probe and endogenous SMN was detected by immunofluorescence (1 experiment, 8 cells). (c) A_T -U1 snRNA colocalizes with transiently transfected GFP-SMN after treatment of cells with Thapsigargin. A_T -U1 snRNA was visualized via an A_T aptamer specific probe and SMN was detected by GFP fluorescence (1 experiment, 57 cells). Scale bar = 5 μ m.



Supplementary Figure 18

Cbl-5xPEG-ATTO 590 does not colocalize to GFP-SMN puncta in the absence of A_T-U1 snRNA. HeLa cells were transiently transfected with a plasmid to produce GFP-SMN, treated with Thapsigargin and loaded with Cbl-5xPEG-ATTO 590. In the absence of a co-transfected plasmid to produce A_T-U1 snRNA, the probe does not accumulate in the puncta marked with GFP (compare with Fig. 3f) (3 experiments, 6 cells). Scale bar = 5 μm.



Supplementary Figure 19

Plasmid maps for A_T-tagged RNA used in this study. (a) Plasmids for production of mRNA fusions. (b) Plasmids for production of U1 snRNA.

Supplementary Tables

Supplementary Table 1

Photophysical properties of fluorophores, probes and Cbl. The extinction coefficients are provided by the manufacturer of the fluorophores. Fluorophores and probes were excited at the excitation λ listed and emission was collected in the range listed below, unless otherwise noted.

| Name | Extinction coefficient ϵ [L mol ⁻¹ cm ⁻¹] (source) | Excitation λ | Emission range |
|--------------------|---|----------------------|----------------|
| FAM | 80,000 (490 nm) (Lumiprobe) | 488 nm | 503 - 660 nm |
| Cbl-FAM | 80,000 (490 nm) (Lumiprobe) | 488 nm | 503 - 660 nm |
| Cbl-C6-FAM | 80,000 (490 nm) (Lumiprobe) | 488 nm | 503 - 660 nm |
| Cbl-1xPEG-FAM | 80,000 (490 nm) (Lumiprobe) | 488 nm | 503 - 660 nm |
| Cbl-2xPEG-FAM | 80,000 (490 nm) (Lumiprobe) | 488 nm | 503 - 660 nm |
| Cbl-3xPEG-FAM | 80,000 (490 nm) (Lumiprobe) | 488 nm | 503 - 660 nm |
| ATTO 488 | 90,000 (501 nm) (Atto tec) | 501 nm | 511 - 700 nm |
| Cbl-C6-ATTO488 | 90,000 (501 nm) (Atto tec) | 501 nm | 511 - 700 nm |
| ATTO 590 | 120,000 (594 nm) (Atto tec) | 594 nm | 604 - 820 nm |
| Cbl-ATTO 590 | 120,000 (594 nm) (Atto tec) | 594 nm | 604 - 820 nm |
| Cbl-C6-ATTO 590 | 120,000 (594 nm) (Atto tec) | 594 nm | 604 - 820 nm |
| Cbl-5xPEG-ATTO 590 | 120,000 (594 nm) (Atto tec) | 594 nm | 604 - 820 nm |
| ATTO 633 | 130,000 (629 nm) (Atto tec) | 629 nm | 639 - 850 nm |
| Cbl-ATTO 633 | 130,000 (629 nm) (Atto tec) | 629 nm | 639 - 850 nm |
| Cbl-C6-ATTO 633 | 130,000 (629 nm) (Atto tec) | 629 nm | 639 - 850 nm |
| Cy5 | 271,000 (646 nm) (Lumiprobe) | 646 nm | 656 - 800 nm |
| Cbl-Cy5 | 271,000 (646 nm) (Lumiprobe) | 646 nm | 656 - 800 nm |
| Cbl | 27,642.26 (361 nm) | | |

Supplementary Table 2

Theoretical estimates of parameters for energy transfer between Cbl absorbance and fluorescence emission of each fluorophore.

| Fluorophore | Overlap integral $J(\lambda)$ between fluorescence emission and Cbl absorbance | Quantum yield Q of fluorophore (source) | Förster distance R_0 |
|-------------|---|--|------------------------|
| FAM | $1.374 \times 10^{14} \text{ nm}^4 \text{ M}^{-1} \text{ cm}^{-1}$ | 0.93 (Lumiprobe) | 35 Å |
| ATTO 488 | $1.424 \times 10^{14} \text{ nm}^4 \text{ M}^{-1} \text{ cm}^{-1}$ | 0.80 (Atto tec) | 35 Å |
| ATTO 590 | $5.266 \times 10^{12} \text{ nm}^4 \text{ M}^{-1} \text{ cm}^{-1}$ | 0.80 (Atto tec) | 20 Å |
| ATTO 633 | $1.026 \times 10^{12} \text{ nm}^4 \text{ M}^{-1} \text{ cm}^{-1}$ | 0.64 (Atto tec) | 15 Å |
| Cy5 | $7.638 \times 10^{11} \text{ nm}^4 \text{ M}^{-1} \text{ cm}^{-1}$ | 0.28 (Lumiprobe) | 12 Å |

Supplementary Table 3

Estimates of linker lengths.

| Name of linker | Estimated length (values for PEG linkers published by ThermoFisher Scientific) |
|----------------|--|
| C6 | 3.5 Å (estimated to be similar to 1xPEG) |
| 1xPEG | 3.5 Å |
| 2xPEG | 7.0 Å |
| 3xPEG | 10.5 Å |
| 5xPEG | 17.5 Å |

Supplementary Table 4

Comparison of maximal distance between the corrin ring in Cbl and the fluorophore in probes. Values are based on structural estimates and the Förster distance R_0 estimated from spectral properties.

| Name | Distance estimate between corrin ring and click linkage to fluorophore | Förster distance R_0 |
|--------------------|--|------------------------|
| Cbl-FAM | 9 Å | 35 Å |
| Cbl-C6-FAM | 12.5 Å | |
| Cbl-1xPEG-FAM | 12.5 Å | |
| Cbl-2xPEG-FAM | 16 Å | |
| Cbl-3xPEG-FAM | 19.5 Å | |
| Cbl-C6-ATTO488 | 12.5 Å | 35 Å |
| Cbl-ATTO 590 | 9 Å | 20 Å |
| Cbl-C6-ATTO 590 | 12.5 Å | |
| Cbl-5xPEG-ATTO 590 | 26.5 Å | |
| Cbl-ATTO 633 | 9 Å | 15 Å |
| Cbl-C6-ATTO 633 | 12.5 Å | |
| Cbl-Cy5 | 9 Å | 12 Å |

Supplementary Table 5

Sequence and properties of DNA oligos used in FISH.

| Name | Sequence | Melting temperature (IDT) | amount used per cover slip |
|-------------------------------|---|---------------------------|----------------------------|
| ACTB-FISH-Cy5 | 5'-Cy5-CAC AGC TTC TCC TTA ATG TCA CGC ACG ATT TCC CGC TCG GCC GTG-3' | 71.1°C | 300 ng |
| A _T -FISH-Cy5 | 5'-Cy5-CCT AGG TGG CAT TCG GAG TAT AAC CGT ATC AAG TAA TCT G-3' | 63.3°C | 200-300 ng |
| A _T -FISH-Alexa546 | 5'-Alexa546-CCT AGG TGG CAT TCG GAG TAT AAC CGT ATC AAG TAA TCT G-3' | 63.3°C | 300 ng |
| U1-FISH-Cy5 | 5'-Cy5-TCA GCA CAT CCG GAG TGC AAT GGA TAA GCC TCG CCC TGG GAA AA-3' | 71.3°C | 200-300 ng |